

Search for Gluinos and Scalar Quarks in $p\bar{p}$ Collisions at $\sqrt{s} = 1.8$ TeV using the Missing Energy plus Multijets Signature

(Dated: October 27, 2018)

We have performed a search for gluinos (\tilde{g}) and squarks (\tilde{q}) in a data sample of 84 pb^{-1} of $p\bar{p}$ collisions at $\sqrt{s} = 1.8$ TeV, recorded by the Collider Detector at Fermilab, by investigating the final state of large missing transverse energy and 3 or more jets, a characteristic signature in R -parity-conserving supersymmetric models. The analysis has been performed ‘blind’, in that the inspection of the signal region is made only after the predictions from Standard Model backgrounds have been calculated. Comparing the data with predictions of constrained supersymmetric models, we exclude gluino masses below $195 \text{ GeV}/c^2$ (95% C.L.), independent of the squark mass. For the case $m_{\tilde{q}} \approx m_{\tilde{g}}$, gluino masses below $300 \text{ GeV}/c^2$ are excluded.

PACS number(s):14.80.Ly, 12.60.-i, 12.60.Jv, 13.85.Rm, 05.45.Jn

T. Affolder,²³ H. Akimoto,⁴⁵ A. Akopian,³⁷ M. G. Albrow,¹¹ P. Amaral,⁸ D. Amidei,²⁵ K. Anikeev,²⁴ J. Antos,¹ G. Apollinari,¹¹ T. Arisawa,⁴⁵ A. Artikov,⁹ T. Asakawa,⁴³ W. Ashmanskas,⁸ F. Azfar,³⁰ P. Azzi-Bacchetta,³¹ N. Bacchetta,³¹ H. Bachacou,²³ S. Bailey,¹⁶ P. de Barbaro,³⁶ A. Barbaro-Galtieri,²³ V. E. Barnes,³⁵ B. A. Barnett,¹⁹ S. Baroiant,⁵ M. Barone,¹³ G. Bauer,²⁴ F. Bedeschi,³³ S. Belforte,⁴² W. H. Bell,¹⁵ G. Bellettini,³³ J. Bellinger,⁴⁶ D. Benjamin,¹⁰ J. Bensinger,⁴ A. Beretvas,¹¹ J. P. Berge,¹¹ J. Berryhill,⁸ A. Bhatti,³⁷ M. Binkley,¹¹ D. Bisello,³¹ M. Bishai,¹¹ R. E. Blair,² C. Blocker,⁴ K. Bloom,²⁵ B. Blumenfeld,¹⁹ S. R. Blusk,³⁶ A. Bocci,³⁷ A. Bodek,³⁶ W. Bokhari,³² G. Bolla,³⁵ Y. Bonushkin,⁶ D. Bortoletto,³⁵ J. Boudreau,³⁴ A. Brandl,²⁷ S. van den Brink,¹⁹ C. Bromberg,²⁶ M. Brozovic,¹⁰ E. Brubaker,²³ N. Bruner,²⁷ E. Buckley-Geer,¹¹ J. Budagov,⁹ H. S. Budd,³⁶ K. Burkett,¹⁶ G. Busetto,³¹ A. Byon-Wagner,¹¹ K. L. Byrum,² S. Cabrera,¹⁰ P. Calafiura,²³ M. Campbell,²⁵ W. Carithers,²³ J. Carlson,²⁵ D. Carlsmith,⁴⁶ W. Caskey,⁵ A. Castro,³ D. Cauz,⁴² A. Cerri,³³ A. W. Chan,¹ P. S. Chang,¹ P. T. Chang,¹ J. Chapman,²⁵ C. Chen,³² Y. C. Chen,¹ M. -T. Cheng,¹ M. Chertok,⁵ G. Chiarelli,³³ I. Chirikov-Zorin,⁹ G. Chlachidze,⁹ F. Chlebana,¹¹ L. Christofek,¹⁸ M. L. Chu,¹ Y. S. Chung,³⁶ C. I. Ciobanu,²⁸ A. G. Clark,¹⁴ A. Connolly,²³ J. Conway,³⁸ M. Cordelli,¹³ J. Cranshaw,⁴⁰ R. Cropp,⁴¹ R. Culbertson,¹¹ D. Dagenhart,⁴⁴ S. D’Auria,¹⁵ F. DeJongh,¹¹ S. Dell’Agnello,¹³ M. Dell’Orso,³³ L. Demortier,³⁷ M. Deninno,³ P. F. Derwent,¹¹ T. Devlin,³⁸ J. R. Dittmann,¹¹ A. Dominguez,²³ S. Donati,³³ J. Done,³⁹ M. D’Onofrio,³³ T. Dorigo,¹⁶

N. Eddy,¹⁸ K. Einsweiler,²³ J. E. Elias,¹¹ E. Engels, Jr.,³⁴ R. Erbacher,¹¹ D. Errede,¹⁸ S. Errede,¹⁸ Q. Fan,³⁶ R. G. Feild,⁴⁷ J. P. Fernandez,¹¹ C. Ferretti,³³ R. D. Field,¹² I. Fiori,³ B. Flaughner,¹¹ G. W. Foster,¹¹ M. Franklin,¹⁶ J. Freeman,¹¹ J. Friedman,²⁴ H. J. Frisch,⁸ Y. Fukui,²² I. Furic,²⁴ S. Galeotti,³³ A. Gallas,^(**) 16 M. Gallinaro,³⁷ T. Gao,³² M. Garcia-Sciveres,²³ A. F. Garfinkel,³⁵ P. Gatti,³¹ C. Gay,⁴⁷ D. W. Gerdes,²⁵ P. Giannetti,³³ P. Giromini,¹³ V. Glagolev,⁹ D. Glenzinski,¹¹ M. Gold,²⁷ J. Goldstein,¹¹ I. Gorelov,²⁷ A. T. Goshaw,¹⁰ Y. Gotra,³⁴ K. Goulios,³⁷ C. Green,³⁵ G. Grim,⁵ P. Gris,¹¹ L. Groer,³⁸ C. Grosso-Pilcher,⁸ M. Guenther,³⁵ G. Guillian,²⁵ J. Guimaraes da Costa,¹⁶ R. M. Haas,¹² C. Haber,²³ S. R. Hahn,¹¹ C. Hall,¹⁶ T. Handa,¹⁷ R. Handler,⁴⁶ W. Hao,⁴⁰ F. Happacher,¹³ K. Hara,⁴³ A. D. Hardman,³⁵ R. M. Harris,¹¹ F. Hartmann,²⁰ K. Hatakeyama,³⁷ J. Hauser,⁶ J. Heinrich,³² A. Heiss,²⁰ M. Herndon,¹⁹ C. Hill,⁵ K. D. Hoffman,³⁵ C. Holck,³² R. Hollebeek,³² L. Holloway,¹⁸ R. Hughes,²⁸ J. Huston,²⁶ J. Huth,¹⁶ H. Ikeda,⁴³ J. Incandela,¹¹ G. Introzzi,³³ J. Iwai,⁴⁵ Y. Iwata,¹⁷ E. James,²⁵ M. Jones,³² U. Joshi,¹¹ H. Kambara,¹⁴ T. Kamon,³⁹ T. Kaneko,⁴³ K. Karr,⁴⁴ H. Kasha,⁴⁷ Y. Kato,²⁹ T. A. Keaffaber,³⁵ K. Kelley,²⁴ M. Kelly,²⁵ R. D. Kennedy,¹¹ R. Kephart,¹¹ D. Khazins,¹⁰ T. Kikuchi,⁴³ B. Kilminster,³⁶ B. J. Kim,²¹ D. H. Kim,²¹ H. S. Kim,¹⁸ M. J. Kim,²¹ S. B. Kim,²¹ S. H. Kim,⁴³ Y. K. Kim,²³ M. Kirby,¹⁰ M. Kirk,⁴ L. Kirsch,⁴ S. Klimenko,¹² P. Koehn,²⁸ K. Kondo,⁴⁵ J. Konigsberg,¹² A. Korn,²⁴ A. Korytov,¹² E. Kovacs,² J. Kroll,³² M. Kruse,¹⁰ S. E. Kuhlmann,² K. Kurino,¹⁷ T. Kuwabara,⁴³ A. T. Laasanen,³⁵ N. Lai,⁸ S. Lami,³⁷ S. Lammel,¹¹ J. Lancaster,¹⁰ M. Lancaster,²³

R. Lander,⁵ A. Lath,³⁸ G. Latino,³³ T. LeCompte,²
 A. M. Lee IV,¹⁰ K. Lee,⁴⁰ S. Leone,³³ J. D. Lewis,¹¹
 M. Lindgren,⁶ T. M. Liss,¹⁸ J. B. Liu,³⁶ Y. C. Liu,¹
 D. O. Litvintsev,¹¹ O. Lobban,⁴⁰ N. Lockyer,³²
 J. Loken,³⁰ M. Loreti,³¹ D. Lucchesi,³¹ P. Lukens,¹¹
 S. Lusin,⁴⁶ L. Lyons,³⁰ J. Lys,²³ R. Madrak,¹⁶
 K. Maeshima,¹¹ P. Maksimovic,¹⁶ L. Malferrari,³
 M. Mangano,³³ M. Mariotti,³¹ G. Martignon,³¹
 A. Martin,⁴⁷ J. A. J. Matthews,²⁷ J. Mayer,⁴¹
 P. Mazzanti,³ K. S. McFarland,³⁶ P. McIntyre,³⁹
 E. McKigney,³² M. Menguzzato,³¹ A. Menzione,³³
 C. Mesropian,³⁷ A. Meyer,¹¹ T. Miao,¹¹ R. Miller,²⁶
 J. S. Miller,²⁵ H. Minato,⁴³ S. Miscetti,¹³
 M. Mishina,²² G. Mitselmakher,¹² N. Moggi,³
 E. Moore,²⁷ R. Moore,²⁵ Y. Morita,²² T. Moulik,³⁵
 M. Mulhearn,²⁴ A. Mukherjee,¹¹ T. Muller,²⁰
 A. Munar,³³ P. Murat,¹¹ S. Murgia,²⁶ J. Nachtman,⁶
 V. Nagaslaev,⁴⁰ S. Nahn,⁴⁷ H. Nakada,⁴³ I. Nakano,¹⁷
 C. Nelson,¹¹ T. Nelson,¹¹ C. Neu,²⁸ D. Neuberger,²⁰
 C. Newman-Holmes,¹¹ C.-Y. P. Ngan,²⁴ H. Niu,⁴
 L. Nodulman,² A. Nomerotski,¹² S. H. Oh,¹⁰
 Y. D. Oh,²¹ T. Ohmoto,¹⁷ T. Ohsugi,¹⁷ R. Oishi,⁴³
 T. Okusawa,²⁹ J. Olsen,⁴⁶ W. Orejudos,²³
 C. Pagliarone,³³ F. Palmonari,³³ R. Paoletti,³³
 V. Papadimitriou,⁴⁰ D. Partos,⁴ J. Patrick,¹¹
 G. Pauletta,⁴² M. Paulini,^(*) ²³ C. Paus,²⁴
 L. Pescara,³¹ T. J. Phillips,¹⁰ G. Piacentino,³³
 K. T. Pitts,¹⁸ A. Pompos,³⁵ L. Pondrom,⁴⁶ G. Pope,³⁴
 M. Popovic,⁴¹ F. Prokoshin,⁹ J. Proudfoot,²
 F. Ptohos,¹³ O. Pukhov,⁹ G. Punzi,³³ A. Rakitine,²⁴
 F. Ratnikov,³⁸ D. Reher,²³ A. Reichold,³⁰
 A. Ribon,³¹ W. Riegler,¹⁶ F. Rimondi,³ L. Ristori,³³
 M. Riveline,⁴¹ W. J. Robertson,¹⁰ A. Robinson,⁴¹
 T. Rodrigo,⁷ S. Rolli,⁴⁴ L. Rosenson,²⁴ R. Roser,¹¹
 R. Rossin,³¹ A. Roy,³⁵ A. Ruiz,⁷ A. Safonov,¹²
 R. St. Denis,¹⁵ W. K. Sakamoto,³⁶ D. Saltzberg,⁶
 C. Sanchez,²⁸ A. Sansoni,¹³ L. Santi,⁴² H. Sato,⁴³
 P. Savard,⁴¹ P. Schlabach,¹¹ E. E. Schmidt,¹¹
 M. P. Schmidt,⁴⁷ M. Schmidt,^(**) ¹⁶ L. Scodellaro,³¹
 A. Scott,⁶ A. Scribano,³³ S. Segler,¹¹ S. Seidel,²⁷
 Y. Seiya,⁴³ A. Semenov,⁹ F. Semeria,³ T. Shah,²⁴
 M. D. Shapiro,²³ P. F. Shepard,³⁴ T. Shibayama,⁴³
 M. Shimojima,⁴³ M. Shochet,⁸ A. Sidoti,³¹
 J. Siegrist,²³ A. Sill,⁴⁰ P. Sinervo,⁴¹ P. Singh,¹⁸
 A. J. Slaughter,⁴⁷ K. Sliwa,⁴⁴ C. Smith,¹⁹
 F. D. Snider,¹¹ A. Solodsky,³⁷ J. Spalding,¹¹
 T. Speer,¹⁴ P. Sphicas,²⁴ F. Spinella,³³ M. Spiropulu,¹⁶
 L. Spiegel,¹¹ J. Steele,⁴⁶ A. Stefanini,³³ J. Strologas,¹⁸
 F. Strumia,¹⁴ D. Stuart,¹¹ K. Sumorok,²⁴ T. Suzuki,⁴³
 T. Takano,²⁹ R. Takashima,¹⁷ K. Takikawa,⁴³
 P. Tamburello,¹⁰ M. Tanaka,⁴³ B. Tannenbaum,⁶
 M. Tecchio,²⁵ R. Tesarek,¹¹ P. K. Teng,¹ K. Terashi,³⁷
 S. Tether,²⁴ A. S. Thompson,¹⁵ R. Thurman-

Keup,² P. Tipton,³⁶ S. Tkaczyk,¹¹ D. Toback,³⁹
 K. Tollefson,³⁶ A. Tollestrup,¹¹ D. Tonelli,³³
 H. Toyoda,²⁹ W. Trischuk,⁴¹ J. F. de Troconiz,¹⁶
 J. Tseng,²⁴ N. Turini,³³ F. Ukegawa,⁴³ T. Vaiciulis,³⁶
 J. Valls,³⁸ S. Vejcik III,¹¹ G. Velev,¹¹ G. Veramendi,²³
 R. Vidal,¹¹ I. Vila,⁷ R. Vilar,⁷ I. Volobouev,²³
 M. von der Mey,⁶ D. Vucinic,²⁴ R. G. Wagner,²
 R. L. Wagner,¹¹ N. B. Wallace,³⁸ Z. Wan,³⁸
 C. Wang,¹⁰ M. J. Wang,¹ B. Ward,¹⁵ S. Waschke,¹⁵
 T. Watanabe,⁴³ D. Waters,³⁰ T. Watts,³⁸ R. Webb,³⁹
 H. Wenzel,²⁰ W. C. Wester III,¹¹ A. B. Wicklund,²
 E. Wicklund,¹¹ T. Wilkes,⁵ H. H. Williams,³²
 P. Wilson,¹¹ B. L. Winer,²⁸ D. Winn,²⁵ S. Wolbers,¹¹
 D. Wolinski,²⁵ J. Wolinski,²⁶ S. Wolinski,²⁵ S. Worm,²⁷
 X. Wu,¹⁴ J. Wyss,³³ W. Yao,²³ G. P. Yeh,¹¹ P. Yeh,¹
 J. Yoh,¹¹ C. Yosef,²⁶ T. Yoshida,²⁹ I. Yu,²¹ S. Yu,³²
 Z. Yu,⁴⁷ A. Zanetti,⁴² F. Zetti,²³ and S. Zucchelli³

(CDF Collaboration)

- ¹ *Institute of Physics, Academia Sinica, Taipei, Taiwan 11529, Republic of China*
- ² *Argonne National Laboratory, Argonne, Illinois 60439*
- ³ *Istituto Nazionale di Fisica Nucleare, University of Bologna, I-40127 Bologna, Italy*
- ⁴ *Brandeis University, Waltham, Massachusetts 02254*
- ⁵ *University of California at Davis, Davis, California 95616*
- ⁶ *University of California at Los Angeles, Los Angeles, California 90024*
- ⁷ *Instituto de Fisica de Cantabria, CSIC-University of Cantabria, 39005 Santander, Spain*
- ⁸ *Enrico Fermi Institute, University of Chicago, Chicago, Illinois 60637*
- ⁹ *Joint Institute for Nuclear Research, RU-141980 Dubna, Russia*
- ¹⁰ *Duke University, Durham, North Carolina 27708*
- ¹¹ *Fermi National Accelerator Laboratory, Batavia, Illinois 60510*
- ¹² *University of Florida, Gainesville, Florida 32611*
- ¹³ *Laboratori Nazionali di Frascati, Istituto Nazionale di Fisica Nucleare, I-00044 Frascati, Italy*
- ¹⁴ *University of Geneva, CH-1211 Geneva 4, Switzerland*
- ¹⁵ *Glasgow University, Glasgow G12 8QQ, United Kingdom*
- ¹⁶ *Harvard University, Cambridge, Massachusetts 02138*
- ¹⁷ *Hiroshima University, Higashi-Hiroshima 724, Japan*
- ¹⁸ *University of Illinois, Urbana, Illinois 61801*
- ¹⁹ *The Johns Hopkins University, Baltimore, Maryland 21218*
- ²⁰ *Institut für Experimentelle Kernphysik, Universität Karlsruhe, 76128 Karlsruhe, Germany*
- ²¹ *Center for High Energy Physics: Kyungpook National University, Taegu 702-701; Seoul National University, Seoul 151-742; and SungKyunKwan University, Suwon 440-746; Korea*

- ²² *High Energy Accelerator Research Organization (KEK), Tsukuba, Ibaraki 305, Japan*
- ²³ *Ernest Orlando Lawrence Berkeley National Laboratory, Berkeley, California 94720*
- ²⁴ *Massachusetts Institute of Technology, Cambridge, Massachusetts 02139*
- ²⁵ *University of Michigan, Ann Arbor, Michigan 48109*
- ²⁶ *Michigan State University, East Lansing, Michigan 48824*
- ²⁷ *University of New Mexico, Albuquerque, New Mexico 87131*
- ²⁸ *The Ohio State University, Columbus, Ohio 43210*
- ²⁹ *Osaka City University, Osaka 588, Japan*
- ³⁰ *University of Oxford, Oxford OX1 3RH, United Kingdom*
- ³¹ *Universita di Padova, Istituto Nazionale di Fisica Nucleare, Sezione di Padova, I-35131 Padova, Italy*
- ³² *University of Pennsylvania, Philadelphia, Pennsylvania 19104*
- ³³ *Istituto Nazionale di Fisica Nucleare, University and Scuola Normale Superiore of Pisa, I-56100 Pisa, Italy*
- ³⁴ *University of Pittsburgh, Pittsburgh, Pennsylvania 15260*
- ³⁵ *Purdue University, West Lafayette, Indiana 47907*
- ³⁶ *University of Rochester, Rochester, New York 14627*
- ³⁷ *Rockefeller University, New York, New York 10021*
- ³⁸ *Rutgers University, Piscataway, New Jersey 08855*
- ³⁹ *Texas A&M University, College Station, Texas 77843*
- ⁴⁰ *Texas Tech University, Lubbock, Texas 79409*
- ⁴¹ *Institute of Particle Physics, University of Toronto, Toronto M5S 1A7, Canada*
- ⁴² *Istituto Nazionale di Fisica Nucleare, University of Trieste/Udine, Italy*
- ⁴³ *University of Tsukuba, Tsukuba, Ibaraki 305, Japan*
- ⁴⁴ *Tufts University, Medford, Massachusetts 02155*
- ⁴⁵ *Waseda University, Tokyo 169, Japan*
- ⁴⁶ *University of Wisconsin, Madison, Wisconsin 53706*
- ⁴⁷ *Yale University, New Haven, Connecticut 06520*
- (*) *Now at Carnegie Mellon University, Pittsburgh, Pennsylvania 15213*
- (**) *Now at Northwestern University, Evanston, Illinois 60208*

The Standard Model (SM) [1] accurately describes physical phenomena down to scales of $\sim 10^{-16}$ cm. There are many extensions of the Standard Model to smaller length scales, including extra gauge interactions, new matter, new levels of compositeness, and supersymmetry (SUSY). Of these, supersymmetry [2] treats the bosonic and fermionic degrees of freedom equally and provides a robust extension to the Standard Model. For simplicity the *minimal* construction (MSSM) is often used to link SUSY with the Standard Model [3]. The most general MSSM would induce proton decay with a weak-interaction lifetime; to avoid this, baryon and lepton conservation are enforced in the MSSM by postulating a new conserved quantity, R -parity, $R = (-1)^{3(B-L)+2s}$, where for each particle s is the spin, and B and L are the respective

baryon and lepton assignments. R -parity conservation leads to characteristic SUSY signatures with missing transverse energy in the final state due to the stable lightest supersymmetric particle (LSP). We assume in the search described below for the bosonic partners of quarks (squarks) and the fermionic partners of gluons (gluinos) that the LSP is weakly interacting, as is the case for most of the MSSM parameter space.

We consider gluino and squark production within the minimal supergravity model (mSUGRA)[3]. In this model the entire SUSY mass spectrum is essentially determined by only five unknown parameters: the common scalar mass at the GUT scale, M_0 ; the common gaugino mass at the GUT scale, $M_{1/2}$; the common trilinear coupling at the GUT scale, A_0 ; the sign of the Higgsino mixing parameter, $sign(\mu)$; and the ratio of the Higgs vacuum expectation values, $\tan\beta$. Minimal SUGRA does not make predictions for the part of the $m_{\tilde{q}}-m_{\tilde{g}}$ mass parameter space where squarks of the first two families are lighter than about 0.8 times the mass of the gluino. Hence for $m_{\tilde{q}} < m_{\tilde{g}}$ we use the constrained MSSM [3] with the set of input parameters being the mass of the gluino, $m_{\tilde{g}}$; the CP -odd neutral scalar Higgs mass, m_A ; the squark masses, $m_{\tilde{q}_i}$; the slepton masses, $m_{\tilde{\ell}_i}$; the squark and slepton mixing parameters, $A_{t(b)(\tau)}$; and μ and $\tan\beta$.

We investigate whether the production and decay of gluinos and scalar quarks is observable in the rate of ≥ 3 -jet events with large missing transverse energy at the Collider Detector at Fermilab (CDF). The large missing energy would originate from the two LSPs in the final states of the squark and gluino decays. The three or more hadronic jets would result from the hadronic decays of the \tilde{q} and/or \tilde{g} . We use the ISAJET Monte Carlo (MC) program [4] with $\tan\beta = 3$ to generate datasets of squark and gluino events, and the PROSPINO program [5] to calculate the production cross sections. To be conservative, only the first two generations of squarks ($\tilde{u}, \tilde{d}, \tilde{c}, \tilde{s}$) are assumed to be produced [6] in the general MSSM framework; we additionally consider production of the bottom squark (\tilde{b}) in the mSUGRA case. The search is based on $84 \pm 4 \text{ pb}^{-1}$ of integrated luminosity recorded with the CDF detector during the 1994-95 Tevatron run.

The CDF detector is described in detail elsewhere [7]. The momenta of charged particles are measured in the central tracking chamber (CTC), which is positioned inside a 1.4 T superconducting solenoidal magnet. Outside the magnet, electromagnetic and hadronic calorimeters arranged in a projective tower geometry cover the pseudorapidity region $|\eta| < 4.2$ [8] and are used to identify jets. Jets are defined as localized energy depositions in the calorimeters and are

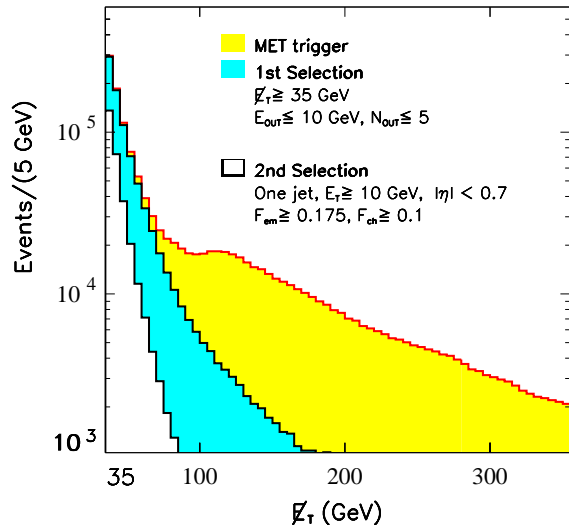


FIG. 1: The \cancel{E}_T spectrum after the online trigger [12] and the two stages of the data preselection. The numbers of events surviving the first and second selections are 892,395 and 286,728, respectively. The variables E_{OUT} , N_{OUT} are energy and number of towers out of time [13].

reconstructed using an iterative clustering algorithm with a fixed cone of radius $\Delta R \equiv \sqrt{\Delta\eta^2 + \Delta\phi^2} = 0.7$ in η - ϕ space [9]. Jets are ordered in transverse energy, $E_T = E \sin \theta$, where E is the scalar sum of energy deposited in the calorimeter towers within the cone, and θ is the angle formed by the beam-line, the event vertex [10], and the cone center.

The missing transverse energy is defined as the negative vector sum of the transverse energy in the electromagnetic and hadronic calorimeters, $\vec{\cancel{E}}_T = -\sum_i (E_i \sin \theta_i) \hat{n}_i$, where E_i is the energy of the i -th tower, \hat{n}_i is a transverse unit vector pointing to the center of each tower, and θ_i is the polar angle of the tower; the sum extends to $|\eta| < 3.6$. The data sample was selected with an on-line trigger which requires $\cancel{E}_T \equiv |\vec{\cancel{E}}_T| > 30$ GeV.

We use a two-stage preselection to reject accelerator- and detector-related backgrounds, beam halo, and cosmic ray events. The first stage is based on timing and energy information in the calorimeter towers to reject events out-of-time with a $p\bar{p}$ collision. The second stage uses the event electromagnetic fraction (F_{em}) and event charged fraction (F_{ch}) to distinguish between real and fake jet events [11]. The preselection requirements and the corresponding missing transverse energy spectra are presented in Figure 1. At least three jets with $E_T \geq 15$ GeV, at least one of them within $|\eta| < 1.1$,

are then required in events that pass the preselection. A total of 107,509 events, predominantly from QCD multijet production, survive the three-jet requirement.

The observed missing energy in QCD jet production is largely a result of jet mismeasurements and detector resolution. In a QCD multijet event with large missing energy, the highest E_T jet is typically the most accurately measured. When the second or third jet is mismeasured because it lands partially in an uninstrumented region (a ‘gap’), the \cancel{E}_T is pulled close in ϕ to the mismeasured jet. A jet is considered non-fiducial if it is within 0.5 rad in ϕ of the \cancel{E}_T direction and also points in η to a detector gap. The second and third highest E_T jets in an event are required to be fiducial. We eliminate the residual QCD component by using the correlation in the $\delta\phi_1 = |\phi_{\text{leading jet}} - \phi_{\cancel{E}_T}|$ versus $\delta\phi_2 = |\phi_{\text{second jet}} - \phi_{\cancel{E}_T}|$ plane. We accept events with $R_1 > 0.75$ rad and $R_2 > 0.5$ rad, where $R_1 = \sqrt{\delta\phi_2^2 + (\pi - \delta\phi_1)^2}$ and $R_2 = \sqrt{\delta\phi_1^2 + (\pi - \delta\phi_2)^2}$.

To avoid potential *a posteriori* biases when searching for new physics in the tails of the missing transverse energy distribution, once we define the signal candidate data sample we make it inaccessible. This analysis approach is often referred to as a ‘blind analysis’ and the signal candidate data sample as a ‘blind box’. The ‘blind box’ data are inspected only after the entire search path has been defined by estimating the total Standard Model backgrounds and optimizing the sensitivity to the supersymmetric signal. We use three variables to define the signal candidate region: \cancel{E}_T , $H_T \equiv E_{T(2)} + E_{T(3)} + \cancel{E}_T$, and isolated track multiplicity, N_{trk}^{iso} [14]. The ‘blind box’ contains events with $\cancel{E}_T \geq 70$ GeV, $H_T \geq 150$ GeV, and $N_{trk}^{iso} = 0$. The large missing transverse energy requirement for the definition of the box is motivated by the requirement that the trigger be fully efficient [13]. The H_T requirement provides good discrimination between signal and background [13]. The N_{trk}^{iso} requirement increases the sensitivity of the search for all-hadronic final states by significantly reducing the backgrounds from W/Z +jets and top-antitop ($t\bar{t}$) events while retaining the signal cascade decays in which a lepton is produced close to a jet (non-isolated lepton). The analysis path is shown in Table I. We reduce the background contribution from $W(\rightarrow e\nu)$ +jets and $t\bar{t}$ production by requiring the two highest energy jets not be purely electromagnetic (jet electromagnetic fraction $f_{em} < 0.9$). We further reduce the contribution from QCD backgrounds (mismeasured jets) by requiring the \cancel{E}_T vector not be closer than 0.3 rad in ϕ to any jet in the event.

We estimate the W and Z boson backgrounds by using a leading order perturbative QCD calculation for $W(Z)$ + jets as implemented in the VEC-

TABLE I: The data selection path for the $\cancel{E}_T + \geq 3$ jets search. After the fourth step, all events that could fall in the ‘blind box’ are removed from the accounting. The events tabulated in the following steps are only in the control bins.

Requirement	Events
Preselection	286,728
$N_{jet} \geq 3$ ($\Delta R = 0.7$, $E_T \geq 15$ GeV)	107,509
Fiducial 2nd, 3rd jet	57,011
$R_1 > 0.75$ rad, $R_2 > 0.5$ rad	23,381
$\cancel{E}_T \geq 70$ GeV, $H_T \geq 150$ GeV, $N_{trk}^{iso} = 0$	‘blind box’
$E_{T(1)} \geq 70$ GeV	
$E_{T(2)} \geq 30$ GeV	
$ \eta (1 \text{ or } 2 \text{ or } 3) < 1.1$	6435
$f_{em(1)}, f_{em(2)} \leq 0.9$	6013
L2 trigger requirement	4679
$\delta\phi_{min}(\cancel{E}_T - jet) \geq 0.3$ rad	2737

BOS Monte Carlo [15], enhanced with a coherent parton shower evolution of both initial- and final-state partons, hadronization, and a soft underlying event model (VECBOS+HERWIG [16]). Events with large missing transverse energy and ≥ 3 jets in the final state are expected primarily from $Z(\rightarrow \nu\bar{\nu}) + \geq 3$ jets and $W(\rightarrow \tau\nu) + \geq 2$ jets (the third jet originating from the hadronic τ decay) processes. The MC predictions for events with ≥ 3 jets are normalized to the observed $Z(\rightarrow ee) +$ jets data sample via the measured $\frac{N_{jet}}{N_{jet}+1}$ ratio, where N_{jet} is the number of jets. The ratio $\rho \equiv \frac{\sigma(pp \rightarrow W(\rightarrow e\nu) + jets)}{\sigma(pp \rightarrow Z(\rightarrow e^+e^-) + jets)}$ is used to normalize the W MC predictions. Assuming lepton universality, the predictions for the number of events with ≥ 2 - and ≥ 3 -jets from W and Z production and decay to all flavors are normalized to the data for $Z(\rightarrow e^+e^-) + \geq 2$ jets. By normalizing the MC predictions to data we avoid large systematic effects due to the renormalization scale, the choice of parton density functions, initial- and final-state radiation, and the jet energy scale. The total uncertainty ($\sim 10\%$) is then dominated by the uncertainty on the luminosity measurement, the uncertainty on the measured ratio $\frac{N_{jet}}{N_{jet}+1}$, and the uncertainty on the predicted ratio ρ as a function of N_{jet} .

We estimate the backgrounds from single top, $t\bar{t}$, and diboson events with Monte Carlo predictions normalized using the respective theoretical cross section calculations for these processes. We generate $t\bar{t}$ events with the PYTHIA MC program [17], normalizing to the fully resummed theoretical cross section $\sigma_{t\bar{t}} = 5.06_{-0.36}^{+0.13}$ pb for $m_{top} = 175$ GeV/ c^2 [18]. We assign a total uncertainty of $\pm 18\%$ on the cross-section to take into account the uncertainty on the top quark mass. The top quark can also be

TABLE II: Comparison of the Standard Model prediction and the data in the bins neighboring bin 8, the ‘blind box’. After the contents of cons were compared in detail to standard model predictions, we ‘opened the box’. We find 74 events in bin 8.

Bin Definition	EWK	QCD	All	Data
$\cancel{E}_T \geq 70, H_T \geq 150, N_{trk}^{iso} > 0$	14	6.3	20 \pm 5	10
$\cancel{E}_T \geq 70, H_T < 150, N_{trk}^{iso} = 0$	2.3	6.3	8.6 \pm 4.5	12
$35 < \cancel{E}_T < 70, H_T > 150, N_{trk}^{iso} = 0$	1.95	135	137 \pm 28	134
$\cancel{E}_T > 70, H_T < 150, N_{trk}^{iso} > 0$	1.73	<0.1	1.73 \pm 0.3	2
$35 < \cancel{E}_T < 70, H_T > 150, N_{trk}^{iso} > 0$	14	9.4	23.4 \pm 6	24
$35 < \cancel{E}_T < 70, H_T < 150, N_{trk}^{iso} = 0$	5	413	418 \pm 69	410
$35 < \cancel{E}_T < 70, H_T < 150, N_{trk}^{iso} > 0$	3.3	28	31 \pm 10	35
$\cancel{E}_T \geq 70, H_T \geq 150, N_{trk}^{iso} = 0$	35	41	76 \pm 13	\square

produced singly via W -gluon fusion and $q\bar{q}$ annihilation with cross sections of $\sigma_{Wg} = 1.7$ pb ($\pm 17\%$), and $\sigma_{W^* \rightarrow t\bar{b}} = 0.73$ pb ($\pm 9\%$) [18]. We use the HERWIG [16] (W -gluon fusion) and PYTHIA ($q\bar{q}$ annihilation) programs to generate the single top production processes. We generate boson pair production with the PYTHIA MC and use the calculated cross sections $\sigma_{WW} = 9.5 \pm 0.7$ pb, $\sigma_{WZ} = 2.6 \pm 0.3$ pb and $\sigma_{ZZ} = 1.0 \pm 0.2$ pb [18].

The data samples we use to study and normalize the QCD Monte Carlo predictions consist of events collected by on-line identification of at least one jet with transverse energy above trigger thresholds of 20 and 50 GeV, and with integrated luminosity of 0.094 pb $^{-1}$ and 2.35 pb $^{-1}$, respectively. The corresponding QCD MC samples are generated using the HERWIG program and a CDF detector simulation. The shapes of the \cancel{E}_T and jet multiplicity distributions are in good agreement with the data, as are the jet kinematic distributions. The QCD predictions are absolutely normalized to the data for $N_{jet} \geq 3$. The total uncertainty on the QCD background estimate is $\sim 15\%$, dominated by a 12% uncertainty due to the detector resolution.

There are seven bins around the ‘blind box’ formed by inverting the requirements which define it (*i.e.* by changing the direction of the inequalities shown in the bin definitions of Table II). We compare the Standard Model background predictions in the bins around the ‘blind box’ with the data. The results are shown in Table II. Of the 35 events from electroweak processes predicted in the ‘blind box’, $\sim 37\%$ are expected from $Z \rightarrow \nu\bar{\nu} + \geq 3$ jets, $\sim 20\%$ from $W \rightarrow \tau\nu + \geq 2$ jets, $\sim 20\%$ from the combined $W \rightarrow e(\mu)\nu_e(\nu_\mu) + \geq 3$ jets, and $\sim 20\%$ from $t\bar{t}$ production and decays. We also compare the kinematic properties between Standard Model predictions and the data around the box and find them to be in agreement [13].

To probe the SUSY parameter space in a simple and

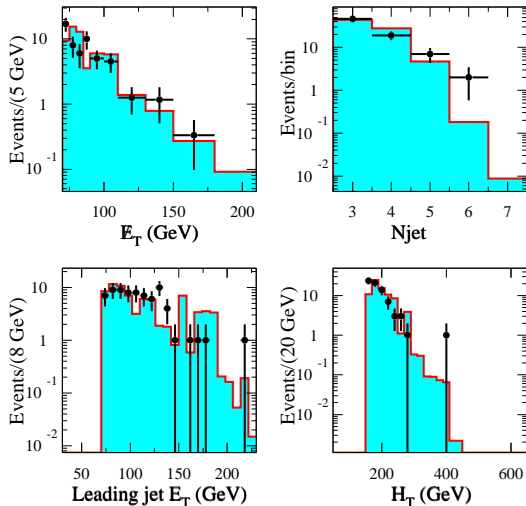


FIG. 2: Comparison in the ‘blind box’ between data (points) and Standard Model predictions (histogram) of \cancel{E}_T , N_{jet} , leading jet E_T and H_T distributions. There are 74 events in each of these plots, to be compared with 76 ± 13 SM predicted events. Note that the \cancel{E}_T distribution is plotted with a variable bin size; the bin contents are normalized as labelled.

comprehensive way we divide the $m_{\tilde{q}} - m_{\tilde{g}}$ plane into four general regions : (A) $m_{\tilde{q}} > m_{\tilde{g}}$ (mSUGRA, five \tilde{q}); (B) $m_{\tilde{q}} \sim m_{\tilde{g}}$ (mSUGRA, five \tilde{q}); (C) $m_{\tilde{q}} < m_{\tilde{g}}$ (MSSM, four \tilde{q}); (D) $m_{\tilde{q}} \ll m_{\tilde{g}}$ (MSSM, four \tilde{q}). We analyze representative points of each region and optimize the \cancel{E}_T and H_T requirements for increased sensitivity to the signal using MC data. The ratio $\frac{N_{SUSY}}{\sqrt{N_{SM}}}$ is maximized in region A for $\cancel{E}_T \geq 90$ GeV and $H_T \geq 160$ GeV; in region B for $\cancel{E}_T \geq 110$ and $H_T \geq 230$ GeV; in C for $\cancel{E}_T \geq 110$ and $H_T \geq 170$ GeV; and in D for $\cancel{E}_T \geq 90$ and $H_T \geq 160$ GeV, where N_{SUSY} is the number of signal events and N_{SM} is the number of Standard Model background events. The signal efficiency ranges between 1% and 14% for the different points in the parameter space, and its total relative systematic uncertainty (mostly due to parton density functions, gluon radiation, renormalization scale and jet energy scale) ranges between 10% and 15%.

In the ‘blind box’, where we expect 76 ± 13 Standard Model events, we observe 74 events. In Figure 2 the predicted Standard Model kinematic distributions are compared with the distributions we observe in the data. For the A/D, B and C region requirements, we observe 31, 5 and 14 events where we expect 33 ± 7 , 3.7 ± 0.5 and 10.6 ± 0.9 events respectively. Based on the

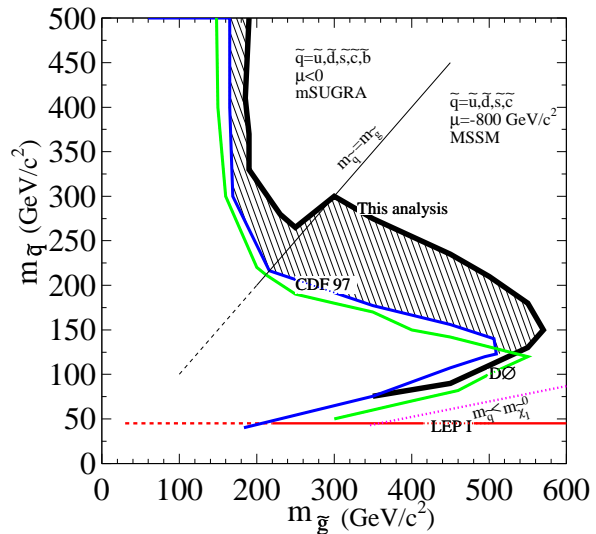


FIG. 3: The 95% C.L. limit curve in the $m_{\tilde{q}} - m_{\tilde{g}}$ plane for $\tan \beta = 3$; the hatched area is newly excluded by this analysis. Results from some previous searches are also shown (CDF [22], DØ [23], LEP I [24]; the area at lower masses in the plane has been previously excluded by the UA1 and UA2 experiments [25, 26]). The region labelled as $m_{\tilde{q}} < m_{\tilde{\chi}_1^0}$ is theoretically forbidden as the squarks are predicted to be lighter than the LSP.

observations, the Standard Model estimates and their uncertainties, and the relative total systematic uncertainty on the signal efficiency, we derive the 95% C.L. [19] upper limit on the number of signal events. The bound is shown on the $m_{\tilde{q}} - m_{\tilde{g}}$ plane in Figure 3. For the signal points generated with mSUGRA the limit is also interpreted in the $M_0 - M_{1/2}$ plane [13]. Studies of the dependence on the value of $\tan \beta$ can be found in [20, 21].

In conclusion, a search for gluinos and squarks in events with large missing energy plus multi-jets excludes at 95% C.L. gluino masses below 300 GeV/c^2 for the case $m_{\tilde{q}} \approx m_{\tilde{g}}$, and below 195 GeV/c^2 , independent of the squark mass, in constrained supersymmetric models. This is a significant extension of previous bounds.

We thank the Fermilab staff and the technical staffs of the participating institutions for their vital contributions. This work was supported by the U.S. Department of Energy and National Science Foundation; the Italian Istituto Nazionale di Fisica Nucleare; the Ministry of Education, Science, Sports and Culture of Japan; the Natural Sciences and Engineering Research Council of Canada; the National Science Council of the

Republic of China; the Swiss National Science Foundation; the A. P. Sloan Foundation; the Bundesministerium fuer Bildung und Forschung, Germany; the Korea Science and Engineering Foundation (KoSEF), the Korea Research Foundation, and the Comision Interministerial de Ciencia y Tecnologia, Spain.

- [1] S. L. Glashow, Nucl. Phys. **22** 588 (1961); S. Weinberg, Phys. Rev. Lett. **19**, 1264 (1967); A. Salam, Proc. 8th Nobel Symposium, Stockholm (1979).
- [2] S. Coleman and J. Mandula, Phys. Rev. **159**, 1251 (1967); P. Ramond, Phys. Rev. **D3**, 2415 (1971); A. H. Chamseddine, R. Arnowitt, and P. Nath, Phys. Rev. Lett. **49**, 970 (1982); Phys. Rev. Lett. **50**, 232 (1983); R. Barbieri, S. Ferrara, and C. A. Savoy, Phys. Lett. **B119**, 343 (1982); L. Hall, J. Lykken and S. Weinberg, Phys. Rev. **D27**, 2359 (1983); H.P. Nilles, Phys. Rept. **110**, 1 (1984).
- [3] For a review, see S. P.Martin, in *Perspectives on supersymmetry*, 1-98, Kane, G.L. (ed.) (1997).
- [4] H. Baer *et al.*, hep-ph/9804321 v7.37 (1998).
- [5] W. Beenakker, R. Hopker, M. Spira, P. M. Zerwas, Nucl. Phys. **B492**, 51 (1997).
- [6] The third generation of squarks can contain states that are lighter than the (assumed degenerate) first and second generation squarks. Alternative search signatures involving *b* and *c* quark tagging are used for scalar bottom and scalar top searches, as in: T. Affolder *et al*, The CDF Collaboration, Phys. Rev. Lett. **85**, 5704 (2000).
- [7] F. Abe *et al.*, Nucl. Inst. and Methods, **A271**, 387 (1988).
- [8] In the CDF coordinate system, ϕ and θ are the azimuthal and polar angles with respect to the proton beam direction. The pseudorapidity η is defined as $-\ln[\tan(\theta/2)]$.
- [9] F. Abe *et al.*, The CDF Collaboration, Phys. Rev. **D45**, 1448 (1992).
- [10] If there are multiple vertices in the event we use the vertex with the largest $\sum p_T$ of associated tracks.
- [11] $F_{em} = \frac{\sum_{j=1}^{N_{jet}} E_{T_j} \times f_{em(j)}}{\sum_{j=1}^{N_{jet}} E_{T_j}}$, where N_{jet} is the number of jets of cone 0.7 with $E_T > 10$ GeV and $f_{em(j)}$ is the Electromagnetic fraction of the *j*-th jet. $F_{ch} = \left\langle \frac{(\sum_i^{tracks} P_{T_i})_j}{E_{T_j}} \right\rangle$ where $(\sum_i^{tracks} P_{T_i})_j$ is the sum of the P_T of all the tracks *i* matched with a central jet *j*.
- [12] The shoulder in the online \cancel{E}_T distribution is due to the contribution of a trigger that requires a jet above 100 GeV.
- [13] M. Spiropulu, Ph.D Thesis, Harvard University (2000).
- [14] N_{trk}^{iso} is the number of high momentum isolated tracks in the event. Tracks qualify as such if they have transverse momentum $P_T \geq 10$ GeV/*c*, impact parameter $d_0 \leq 0.5$ cm, vertex difference $|z_{track} - z_{event}| < 5$ cm and the total transverse momentum ΣP_T of all tracks (with impact parameter $d_0^i \leq 1$ cm) around them in a cone of $\Delta R \equiv \sqrt{\Delta\eta^2 + \Delta\phi^2} = 0.4$ is $\Sigma P_T \leq 2$ GeV/*c*.
- [15] F. A. Berends, W. T. Giele, H. Kuijf, and B. Tausk, Nucl. Phys. **357**, 32 (1991).
- [16] G. Marchesini *et al.*, Comput. Phys. Commun. **67**, 465 (1992). HERWIG v5.6 is used. See hep-ph/9607393 (1996).
- [17] T. Sjöstrand, Comput. Phys. Commun. **82**, 74 (1994). PYTHIA v5.7 is used.
- [18] R. Bonciani *et al.*, Nucl. Phys. **B529**, 424 (1998); T. Stelzer, Z. Sullivan and S. Willenbrock, Phys. Rev. **D54**, 6696 (1996); T. Tait and C. P. Yuan, hep-ph/9710372 (1997); J. Ohnemus *et al.*, Phys. Rev. **D43**, 3626 (1991); Phys. Rev. **D44**, 1403 and 3477 (1991). The measured top cross section (T. Affolder *et al.*, submitted to Phys. Rev. (2001)) is in agreement with the theoretical prediction.
- [19] G. Zech, Nucl. Instrum. Methods **A277**, 608 (1989); T.Huber *et al.*, Phys Rev **D41**, 2709 (1990).
- [20] V. Barger *et al*, hep-ph/0003154 (2000).
- [21] V. Krutelyov *et al*, Phys. Lett. **B505** 161 (2001).
- [22] F. Abe *et al.*, The CDF Collaboration, Phys. Rev. **D56**, R1357 (1997).
- [23] S. Abachi *et al.*, The DØ Collaboration, Phys. Rev. Lett. **75**, 618 (1995).
- [24] P. Abreu *et al.*, The DELPHI Collaboration, Phys. Lett. **B247**, 148 (1990).
- [25] C. Albajar *et al.*, The UA1 Collaboration, Phys. Lett. **B198**, 261 (1987).
- [26] J. Alitti *et al.*, The UA2 Collaboration, Phys. Lett. **B235**, 363 (1990).